

PCCP

Accepted Manuscript



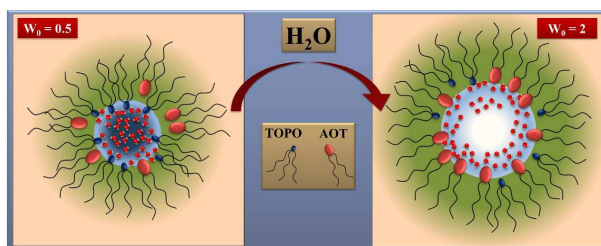
This is an *Accepted Manuscript*, which has been through the Royal Society of Chemistry peer review process and has been accepted for publication.

Accepted Manuscripts are published online shortly after acceptance, before technical editing, formatting and proof reading. Using this free service, authors can make their results available to the community, in citable form, before we publish the edited article. We will replace this *Accepted Manuscript* with the edited and formatted *Advance Article* as soon as it is available.

You can find more information about *Accepted Manuscripts* in the [Information for Authors](#).

Please note that technical editing may introduce minor changes to the text and/or graphics, which may alter content. The journal's standard [Terms & Conditions](#) and the [Ethical guidelines](#) still apply. In no event shall the Royal Society of Chemistry be held responsible for any errors or omissions in this *Accepted Manuscript* or any consequences arising from the use of any information it contains.

Graphical Abstract



Proportion of TOPO in Water/AOT:TOPO/*n*-heptane reverse micelles produces dramatic changes in the water structure, size and composition of the interface.

**How TOPO Affects the Interface of the Novel Mixed Water/AOT:TOPO/*n*-heptane
Reverse Micelles. A Dynamic Light Scattering and Fourier Transform Infrared
Spectroscopy Study**

Emmanuel Odella, R. Darío Falcone, Juana J. Silber, N. Mariano Correa*

*Departamento de Química. Universidad Nacional de Río Cuarto. Agencia Postal # 3. C.P.
X5804BYA Río Cuarto. ARGENTINA*

[*] Dr. N. Mariano Correa. Corresponding-Author,

Departamento de Química. Universidad Nacional de Río Cuarto. Agencia Postal # 3.

C.P. X5804BYA Río Cuarto. ARGENTINA. E-mail: mcorrea@exa.unrc.edu.ar

Lic. Emmanuel Odella, Dr. R. Darío Falcone, Prof. Juana J. Silber,
Departamento de Química. Universidad Nacional de Río Cuarto. Agencia Postal # 3.
C.P. X5804BYA Río Cuarto. ARGENTINA

ABSTRACT

In this work we report for the first time the formation of two reverse micelles (RMs) media created with the nonionic surfactant tri-*n*-octyl phosphine oxide (TOPO) in *n*-heptane and the one created mixing the anionic sodium 1,4-bis-2-ethylhexylsulfosuccinate (AOT) with different TOPO content dissolved in *n*-heptane.

Dynamic light scattering (DLS) experiments, reveal the formation of water/TOPO/*n*-heptane (TOPO RMs) and water/AOT:TOPO/*n*-heptane RMs (mixed RMs) since the droplet sizes values increase as the water content increase. The addition of TOPO to the system at W_0 ($W_0 = [\text{water}] / ([\text{AOT}] + [\text{TOPO}])$) constant, causes the mixed RMs droplet sizes to decrease compared with the AOT RMs. In addition, the decrease is larger when the water content is low ($W_0 = 0.5$) but the effect is negligible at the maximum W_0 value analyzed ($W_0 = 2$). These results are not expected for mixtures of different nonionic surfactants with AOT and were explained considering the unique TOPO structure. Thus, at $W_0 = 0.5$, we suggest that the percentage of TOPO molecules at the mixed RMs interface is higher than the corresponding to the bulk solution. On the other hand, at $W_0 = 2$ the RMs interface is comprised mainly with AOT molecules.

FT-IR experiments performed by monitoring monodeuterated water frequency (ν_{OD}) show in TOPO RMs bound and “bulk-like” water structure even at very low water content. On the other hand, for mixed RMs the water structure depend on the water content. At low W_0 value, there are two kinds of water molecules and at W_0 value around 2 only bound water exists.

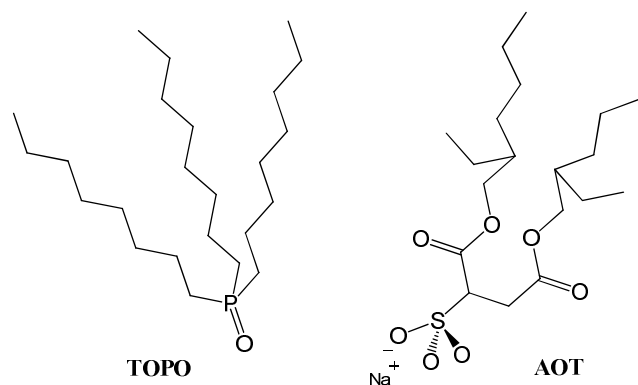
Fourier transform infrared (FT-IR) experiments performed on the symmetric ($\nu_s\text{SO}_3$) and asymmetric ($\nu_a\text{SO}_3$) sulfonate stretching band of AOT reveal the existence of strong $\text{Na}^+\cdot\text{TOPO}$ complex in the mixed RMs.

The results show that adding TOPO to form mixed surfactant RMs with AOT reduces their size, changes the nature of the water to have a “bulk-like” character and diminishes the ion pairing of the sulfonate with Na^+ .

INTRODUCTION

Reverse micelles (RMs) are supramolecular assemblies formed when surfactants are dissolved in nonpolar organic solvents. The surfactant polar or charged groups are located in the interior (core) while their hydrocarbon tails extend into the organic nonpolar media.¹⁻³ Different anionic, cationic and nonionic surfactants have been employed to prepare RMs in nonpolar solvents.¹⁻¹² Among the anionic surfactants that form RMs, the best known is sodium 1,4-bis-2-ethylhexylsulfosuccinate (AOT, Scheme 1) in different solvents. It is known that AOT forms spherical RMs in aromatic and aliphatic solvents without addition of a cosurfactant and, water can be solubilized up to $W_0 = [\text{H}_2\text{O}] / [\text{Surfactant}] \sim 60$ depending on the external solvent and temperature.¹³ Many biophysical applications depend on the magnitude of non-covalent interactions of the RMs interface with specific sites of biological macromolecules solubilized inside.¹³⁻¹⁵ Therefore, the effective control of these interactions may be regulated by changes at the interface due to the addition of a second surfactant. In this sense, it has been found that the addition of nonionic surfactants to the RMs interfaces formed by ionic surfactants produce significant changes in enzyme activities,^{16,17} polymer¹⁸ and nanoparticles synthesis.¹⁹

Previous studies performed on RMs systems involving more than one surfactant have been shown in the literature. Those studies used solubilization,²⁰⁻²² viscosity,²³ spectroscopic,²⁴⁻²⁶ conductivity,^{21,27} SANS,²⁸⁻³⁰ FT-IR spectroscopy and nuclear magnetic resonance (NMR),^{31,32} establishing emphasis on understanding the mixed interface and the structure of the confined water.



Scheme 1: Molecular structure of TOPO and AOT surfactants.

For example, Liu et al.²⁰ studied the solubilization of both water and NaCl aqueous solutions in mixed RMs formed by AOT and nonionic surfactants such as polyoxyethylene glycol alkyl ethers series (Brij's series) in different aliphatic solvents. They found that the maximum amount of water solubilized was enhanced in the presence of a certain concentration of NaCl, and the concentration increases with the content of the nonionic surfactant and the polyoxyethylene chain (EO) length. Furthermore, Mitra and Paul²² studied the mixture of AOT with nonionic surfactants (Brijs, Spans, Tweens, Igepal CO 520), a cationic surfactant dioctadecyl dimethylammonium bromide (DDAB) with nonionic surfactants (Brij's, Spans, Igepal CO 520) and a nonionic surfactant (Igepal CO 520) with nonionic surfactants (Brij's, Spans) in solvents of different chemical structures and physical properties. They found that the maximum water solubilization capacity (W_{0Max}) is obtained at a certain molar fraction of the nonionic surfactant ($X_{nonionic Max}$) and that parameter is dependent on both the content of the nonionic surfactant in the mixture and the length of the EO chains in the polar head.

The addition of a second surfactant also affects the size of these supramolecular systems, which has a direct connection with the water solubilization capacity. Liu et al.³³ investigated the microstructure and conductivity of water/AOT:nonionic surfactants/*n*-heptane and they found that the increase in both the content and the length to the EO chain of Brij's surfactants used, causes an increase in the water solubilization capacity with the consequent increase in the micellar size. Das et al.³⁴ investigated the AOT/Igepal-520/cyclohexane mixed RMs and they found a 5-fold increase in water solubilization capacity compared to that of the constituent surfactants at an Igepal 520 molar fraction of 0.4 and also the micellar size increases.

As summarized, there is clear evidence that the properties of RMs are modified when composed of mixed surfactants. However, to the best of our knowledge, all the studies are performed using nonionic surfactants which have a very long polar part in its moiety, which changes significantly the surfactant packing parameter P_c ($P_c = v/a_0l_c$, where v and l_c are the volume and the length of hydrophobic chain, respectively, and a_0 the area of polar head group of the surfactant).

On the other hand, the nonionic surfactant tri-*n*-octyl phosphine oxide (TOPO, Scheme 1) is a molecule that has a very small polar head (the P=O group) in comparison with its hydrophobic chains.³⁵ Furthermore, TOPO has more than one hydrocarbon tail and distinguishes from those that have only a single tail. Thus, TOPO differs structurally from other conventional nonionic surfactants and has a greater P_c . For example, the Brij's surfactants are characterized by long polar heads which even manage to have the same or larger length than the hydrophobic region.³⁶

In addition, the great versatility in the use of TOPO in different scientific and technological fields lies in the unique properties of the P=O group which contains free pairs of electrons with a strong ability to complex numerous species.³⁷ This feature is implemented, consequently, in the separation and purification of metals.^{38,39} TOPO is one of the most powerful extraction agents of a large number of metal ions.⁴⁰⁻⁴² To verify the best conditions with regard to the formation of complexes, extraction and recovery metals, many studies have been performed to date.⁴³⁻⁴⁹

Furthermore, numerous studies have reported the use of this compound as an alternative for the nanoparticles synthesis, controlling and inhibiting their growth morphology.⁵⁰⁻⁵² Moreover, its use is widely known in preparing quantum dots of InP, CdSe and ZnO in a range of organic solvents.⁵³⁻⁵⁸ Even though the great versatility that TOPO showed in homogeneous and heterogeneous media there are no reports dealing with its properties in microheterogeneous systems such as RMs.

To the best of our knowledge there are no studies that evaluate TOPO alone or mixed with AOT to generate RMs. Therefore, in this work, we have investigated the formation of RMs with water/TOPO/*n*-heptane (TOPO RMs) and water/AOT:TOPO/*n*-heptane (mixed RMs) systems to gain insights into their interfacial properties. Our purpose is to understand the effect that a complexing agent has on the AOT interface to investigate unique interfacial properties of the mixed RMs. To achieve this goal, we have used dynamic light scattering (DLS) to probe the existence of the different RMs media and FT-IR technique to monitor the changes in the several vibration modes of TOPO, AOT and water. Thus, we have studied the carbonyl (C=O) and the symmetric and antisymmetric sulfonate (SO₃⁻) region for the AOT surfactant, the P=O region for TOPO only in the TOPO RMs, and the O-D

region for water. The results show important changes in the mixed RMs interface and the water entrapped properties which depend both on the water content and the TOPO molar fraction. The results show unique properties of the mixed RMs in the sense that bulk water is found even at very low W_0 values and, the water properties can be changed simply by modification of the TOPO content at the interface. These intriguing results may have important application in the use of these systems as nanoreactors, for example in enzymatic catalysis and, polymer and nanoparticles synthesis, venue that we are currently investigating.

EXPERIMENTAL SECTION

Materials

Sodium 1,4-bis (2-ethylhexyl) sulfosuccinate (AOT) from Sigma (> 99% purity) and tri-*n*-octylphosphine oxide (TOPO) from Sigma (> 99% purity) were used as received. Both surfactants were dried under vacuum prior use. The *n*-heptane and CCl_4 from Sigma (HPLC quality), were used without prior purification. Ultrapure water was obtained from Labonco equipment model 90901-01. Monodeuterated water (HOD) was prepared by stirring a solution of 10% D_2O in H_2O at room temperature for 1h in order to allow the exchange of H.

Methods

AOT and TOPO were prepared by mass and volumetric dilution at a concentration of 0.25 M to prepare two stock solutions and then mixed them in the desired proportions in order to obtain the desired mixed RMs concentration. The mole fraction of TOPO, $X_{\text{TOPO}} = [\text{TOPO}] / ([\text{AOT}] + [\text{TOPO}])$ was varied from 0 to 1 in the case of water solubilization

capacity experiments and from 0 to 0.7 for the rest of the experiments in the mixed systems. Aliquots of these stock solutions were used to make individual mixed RMs solutions with different amounts of water, defined as $W_0 = [\text{H}_2\text{O}] / ([\text{AOT}] + [\text{TOPO}])$. The incorporation of water into each micellar solutions was performed using calibrated microsyringes. To obtain optically clear solutions they were shaken in a sonicating bath. The resulting solutions were clear with a single phase and they were used in DLS experiments to determine the RM size. Similar sample preparation was used for FT-IR experiments. The W_0 was varied between 0-2 in the mixed systems and between 0-0.8 in TOPO/*n*-heptane system. The lowest value for W_0 ($W_0 = 0$), corresponds to a system without the water addition.

In all the experiments the total surfactant concentration ($[\text{Surf.}]_{\text{T}} = [\text{AOT}] + [\text{TOPO}]$) was kept constant at 0.2 M. In the FT-IR experiments performed in the C=O and SO_3^- AOT stretching modes the overall concentration was kept constant at 0.05M.

General

Water solubilization capacity of the AOT:TOPO/*n*-heptane systems was determined by titration of a 2 mL surfactants/oil solution by drop wise addition of water followed by vigorous shaking in order to ensure the attainment of complete equilibrium. Appearance of persistent visual turbidity and/or phase separation was considered to be the solubilization limit. Average of three successive measurements was taken as the final result.

The apparent diameters (d_{app}) of the different RMs were determined by dynamic light scattering (DLS, Malvern 4700 with goniometer) with an argon-ion laser operating at 488 nm. All the DLS experiments were carried out at fixed $[\text{Surf.}]_{\text{T}} = 0.2$ M. Thus, the RMs solutions are not at infinite dilution, nevertheless we think appropriate to introduce a d_{app} to

make the comparison of our systems. A similar approach was used by other authors.⁵⁹ Anyway, we have tested the systems at other lower concentrations and the results were the same but the acquisition times were much longer. Thus, we were confident that working at 0.2 M there are no much interdroplet interactions and the data are reproducible. Cleanliness of the cuvettes used for measurements was of crucial importance for obtaining reliable and reproducible data.⁶⁰ Cuvettes were washed with ethanol, and then with doubly distilled water and dried with acetone. Prior to use the samples was filtered three times using an Acrodisc with 0.2 μm PTFE membrane (Sigma) to avoid dust or particles presents in the original solution. Before introducing each sample to the cuvette, it was rinsed with pure *n*-heptane twice and finally with the sample to be analyzed. Prior to the measurements on a given day, the background signals from air and *n*-heptane were collected to confirm cleanliness of the cuvettes. Previous to data acquisition, samples were equilibrated in the DLS instrument for 10 min at 25 °C. Multiple samples at each size were made, and thirty independent size measurements were made for each individual sample at the scattering angle of 90°. The instrument was calibrated before and during the course of experiments using several different size standards. Thus, we are confident that the magnitudes obtained by DLS measurements can be taken as statistically meaningful for all the systems investigated. The algorithm used was CONTIN and the DLS experiments show that the polydispersity of the RMs size is less than 5 %.

FT-IR spectra were recorded with a Nicolet IMPACT 400 spectrometer. The FT-IR measurements for the RMs samples were taken in Irtran-2 cell of 0.5 mm path length from Wilmad Glass (Buena, NJ). FT-IR spectra were obtained by co-adding 200 spectra at a resolution of 0.5 cm^{-1} . For the experiments performed on the C=O and SO_3^- stretching

modes, the *n*-heptane spectrum was used as the background. For the O-D stretching band a different procedure was performed. The ν_{OD} spectral band of HOD was superimposed on a finite background. It was assumed that this background could be approximated with the spectrum of 100% H₂O in the ν_{OD} spectral region.⁶¹⁻⁶³ Therefore the reference sample, at each W_0 values, was a surfactant solution containing exactly the same W_0 but adjusted with pure H₂O. The reason for using partially deuterated water is explained in the results and discussion section. For each spectral deconvolution we have fixed the bandwidth and have used the multiple Gaussian curve fitting procedure to separate the individual peaks using Microcal Origin 8.0 software. We have smoothed the curves for proper fitting where it was necessary and we started the deconvolution until we obtained the satisfactory fitting condition and checked it with the help of prediction and confidence band setting the values at 95 %.⁶²

The FT-IR spectrum of solid TOPO was registered from a pressed disk of the pure TOPO mixed with KBr powder. For the experiments performed on the P=O stretching mode in the TOPO/*n*-heptane and TOPO/CCl₄ systems, the *n*-heptane and CCl₄ spectra were used as the background.

All the experiments were carried out at 25 ± 0.5 °C.

RESULTS AND DISCUSSION

Solubilization of water in water/AOT:TOPO/n-heptane mixed systems.

Figure 1 shows the maximum amount of water (W_{0Max}) as a function of X_{TOPO} that the AOT:TOPO mixed systems can accept giving a transparent and stable single phase. Above this threshold the media becomes cloudy because the phase transition occurs.

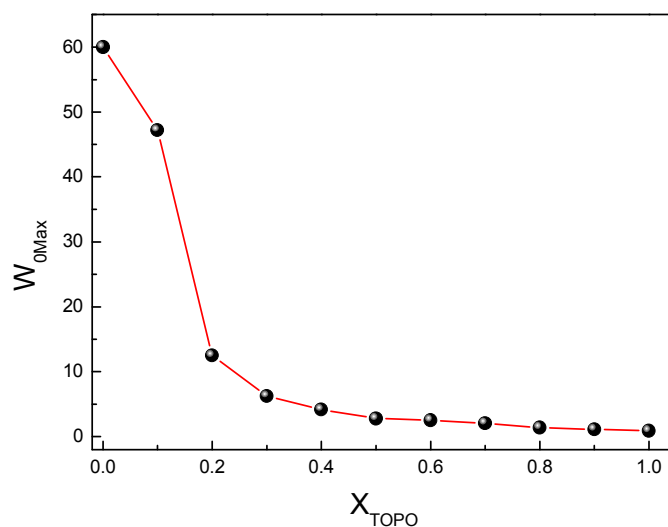


Figure 1: Maximum amount of water solubilized ($W_{0\text{Max}}$) in AOT:TOPO/*n*-heptane mixed systems as a function of X_{TOPO} . $[\text{Surf.}]_{\text{T}} = 0.2 \text{ M}$.

As can be seen, for $X_{\text{TOPO}} = 0$ the $W_{0\text{Max}}$ for the water/AOT/*n*-heptane system is approximately 60, which is consistent with the literature reports.⁶⁴ With the progressive increase of the X_{TOPO} value, the solubilized amount of water decreases dramatically. For the system with the $X_{\text{TOPO}} = 0.2$ the $W_{0\text{Max}}$ is equal to 12.5, showing the reduction of almost 80% in the maximum amount of the water solubilized. When the system consists of an equimolar ratio of the two surfactants ($X_{\text{TOPO}} = 0.5$) the $W_{0\text{Max}}$ is 2.8, and thereafter the profile shown no significant changes. Finally, for the system formed only with TOPO surfactant ($X_{\text{TOPO}} = 1$) the $W_{0\text{Max}}$ is equal to 1. This result is very different than those obtained with other mixed systems where the water content, generally, is higher with the presence of the nonionic surfactant showing synergism in the water solubilization.²⁰⁻²²

Solubilization of water in RMs depends on many factors, for example, on the type of surfactant (and cosurfactant or a second surfactant), oil, temperature, and additives;^{20,34,65} but the main driving force of such solubilization is the spontaneous curvature and the elasticity (or rigidity) of the interfacial film formed by the surfactants and the interdroplet interactions.^{34,66,67} The natural curvature radius is larger and RMs sizes are smaller when the P_c values are larger.⁶⁸ Any factor that increases the P_c , decreases the RMs sizes and consequently, decreases the water solubilization capacity significantly.

For a mixture of surfactants an effective packing parameter (P_{eff}) of the mixed RMs media is defined as Eqn. 1:⁶⁹

$$P_{eff} = (v/a_0l_c)_{eff} = \frac{(x_A v/a_0l_c)_A + (x_B v/a_0l_c)_B}{x_A + x_B} \quad \text{Eqn. 1}$$

where x_A and x_B are the mole fractions of surfactants A and B at the interface respectively. If one of the surfactants is a traditional nonionic surfactants, P_{eff} changes significantly. Many calculations of P_c values, for different types of surfactants⁷⁰ indicate, for example, that the v/a_0l_c value for Brij nonionic surfactants decrease with increasing their EO chains, and generally this ratio is smaller than AOT. Liu et al.³³ studied the conductivity and microstructure of aqueous mixed RMs formed by AOT and nonionic surfactants and they found an increase on micellar size compared to AOT RMs. Such growth was explained by the decrease of P_{eff} caused by the increase both in the content and the long chain EO of the Brij surfactants employed. On the other hand, Mitra et al.⁷¹ studied the dynamics and reactivity of water encapsulated in mixed RMs formed by AOT/Brij-30 in isoctane. The

RMs sizes were analyzed with DLS and they observed a significant increase in size over $X_{\text{Brij-30}} = 0.8$ (molar fraction of Brij-30 in the mixture). The authors attributed this increase to a particular deformation of the aggregates after incorporation of the nonionic surfactant and the hydrophobicity of the hydrocarbon tail.

On the other hand, all the factors that increase the ν values or decrease the a_0 values would increase the P_{eff} value. TOPO has smaller a_0 and larger ν than AOT, and thus on mixing TOPO with AOT, P_{eff} is increased which in turn decreases the droplet size of the RMs system. Thus, AOT:TOPO/*n*-heptane mixed system can solubilize less water than the AOT/*n*-heptane RMs, and with increasing X_{TOPO} value, the solubilization capacity of the mixed system decreases.

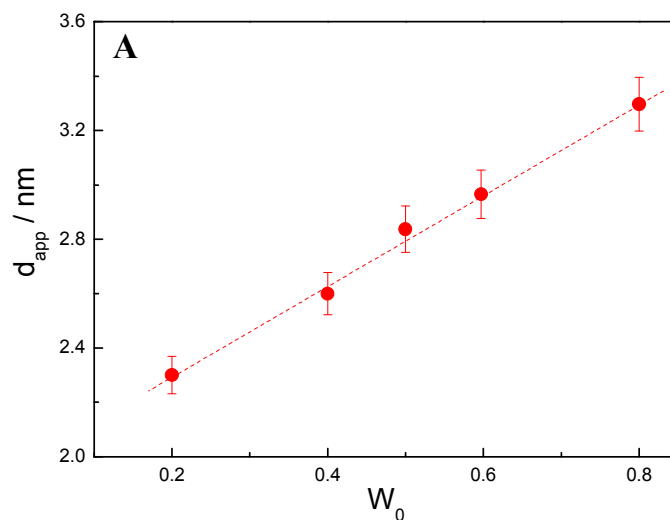
Moreover, experimentally it has been shown that the increase of attractive interactions among the aggregates is associated with an increasing penetrable length of the interfacial region as evidenced from a growing difference between the hard-sphere radius and the hydrodynamic radius.^{64,72} The presence of TOPO molecules in the oil/water interface increases the penetrable length, which would increase the attractive interactions among the droplets and thus decrease the water solubilization capacity accordingly.^{73,74} Meanwhile, the partial replacement of AOT with TOPO molecules decreases the number of the surfactant molecules that self-assemble into aggregates, which further decreases the water solubilization capacity owing that TOPO alone can only solubilize water up to $W_0 = 1$.

DLS experiments

A question may arise here that if the water is effectively encapsulated by the surfactants creating a true mixed RMs media at every TOPO molar fraction investigated.

DLS is used to assess this matter for water/AOT:TOPO/*n*-heptane at different X_{TOPO} , because it is a powerful technique to evaluate the formation of RMs.^{1-3,75-78} Thus, if water is really encapsulated to form mixed RMs, the droplets size must increase as the W_0 increases with a linear tendency (swelling law of RMs) as it is well established for water or polar solvents/surfactant RMs systems.^{2,75,76,79} This feature can also demonstrate that the water/AOT:TOPO/*n*-heptane mixed RMs media consist of discrete droplets.⁷⁶

In Figure 2 we report the d_{app} values obtained in water/AOT:TOPO/*n*-heptane systems for (A) $X_{\text{TOPO}} = 1$ and (B) $X_{\text{TOPO}} = 0, 0.3, 0.5$ and 0.7 , respectively.



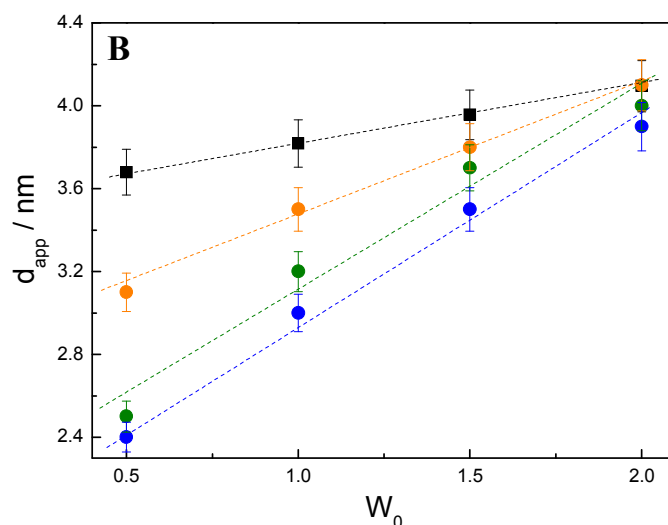


Figure 2: Water/AOT:TOPO/*n*-heptane droplets apparent diameters (d_{app}) as a function of W_0 for (A) $X_{TOPO} = 1$ and (B) $X_{TOPO} = 0$ (■) extrapolated from ref. 12, 0.3 (●), 0.5 (●) and 0.7 (●). $[Surf.]_T = 0.2$ M.

In all the systems studied it can be observed that there is an increase in d_{app} value when the W_0 increases even for the system where TOPO is the only surfactant (Figure 2A). In addition, because there are no reports on TOPO RMs and noting the linear profile in the growth of the aggregates in the whole W_0 range analyzed, we can estimate that they are discrete droplets. The linear tendency observed in Figure 2B shows that water is effectively sequestered by AOT:TOPO/*n*-heptane giving mixed RMs at every X_{TOPO} studied.

The data is analyzed at constant W_0 to investigate the effect of the TOPO addition and it can be seen that the RMs droplet sizes of mixed RMs decrease compared with the AOT RMs (Figure 2B, black squares). In addition, a larger decrease is observed when the water content is low ($W_0 = 0.5$) and is practically negligible at the maximum W_0 value analyzed

($W_0 = 2$). For example, the droplet sizes for $X_{\text{TOPO}} = 0$ at $W_0 = 0.5$ is 3.7 nm, while for $X_{\text{TOPO}} = 0.7$, is 2.4 nm. In contrast, when $W_0 = 2$, d_{app} value is 4.0 nm and 3.9 nm for $X_{\text{TOPO}} = 0$ and 0.7, respectively.

One explanation of the observed phenomenon can be interpreted, among other factors, in terms of increasing the P_{eff} of the mixed systems with the addition of TOPO as it was explained, since the RMs sizes are smaller when the P_{eff} values increase.^{69,80}

Consequently our results are different with what is known from most studies involving traditional nonionic surfactants where adding them to the system increase the ability to solubilize water (or salts) and increases the size.^{22,25,26,34,65} The difference in behavior lies in the unique TOPO structure. First, the three hydrocarbon tails gives to the molecule a large volume in the hydrophobic region. Furthermore, the TOPO polar head is very small and appreciably different from the nonionic surfactants Brij series and TX-100,³⁶ which have long EO chains. Thus, the simultaneous combination of both geometric characteristics shows that the P_c of TOPO is larger than the P_c of AOT and the traditional nonionic surfactants used. Accordingly, the incorporation of TOPO in the interface greatly increases the v_{eff} , and hence the P_{eff} (Eqn. 1) and, leads to decrease the mixed RMs sizes as Figure 2 shows. Similar results were also reported by Bardhan and Paul working with cationic-nonionic mixed RMs.⁸¹ They studied the RMs formed by water/Brij-58:CTAB/1-pentanol/*n*-heptane (or decane) and found that the RMs size decreases with the increase of the nonionic surfactant content in the mixed systems. They argue that the droplet sizes of the mixed RMs is mainly governed by the repulsion between head groups of the surfactants (viz. steric origin for EO head groups and electrostatic origin for quaternary ammonium head groups) and also by the packing parameters of the surfactants forming the mixture.

A careful analysis of the observed differences in sizes varying the TOPO composition when the $W_0 = 0.5$, compared to the $W_0 = 2$ could be explained by investigating the composition of the mixed interface, referring specifically to the distribution and location of the molecules of both surfactants. Since at $W_0 = 0.5$ the increase of TOPO content causes the decrease in the mixed RMs size compared to the size of the AOT RMs (Figure 2B), we believe that when the water content is low, the percentage of TOPO molecules at the mixed RMs interface is higher than the corresponding to the prepared solution. This is equivalent to an increase in the mole fraction of TOPO at the interface (x_{TOPO}), which increases the P_{eff} value according to Eqn. 1, and consequently, decreases the RM size.

On the contrary, at $W_0 = 2$ the sizes of the mixed RMs at different X_{TOPO} do not differ substantially in comparison with the d_{app} values of the RMs formed only with AOT. Thus, we suggest that the micellar interface is composed mostly by AOT molecules.

We also wonder if there could be another reason for the explanation of these results. Apparently, the nature of the encapsulated water could play a crucial role on the control of the size of these mixed aggregates. Our data also could be explained considering differences in the water–surfactant interaction depending on the TOPO content at W_0 value fixed. Particularly at small W_0 values where the interface seems to be rich in TOPO molecules, the experimental results obtained by DLS can also be explained considering an unequal interaction between water and the surfactants at the interface as it will be shown in the FT-IR section.

In summary, the DLS results suggest that at $W_0 = 0.5$, the mixed RMs are small and the micellar interface may be comprised mainly with TOPO surfactant molecules. In contrast, at $W_0 = 2$, the sizes of the mixed RMs are larger than at $W_0 = 0.5$, independent on

the TOPO content and quite similar to the one of RMs formed only with AOT, probably showing that the interface is dominated by the presence of AOT molecules respect to TOPO molecules.

FT-IR study in water/AOT:TOPO/n-heptane mixed Reverse Micelles.

To gain more insights about the mixed RMs composition and the water–surfactant interaction we investigated the system using the noninvasive technique FT-IR spectroscopy which allows us to monitor different vibrational bands and infer interactions present at the interface.⁸²⁻⁸⁵ Thus we follow the water O-D stretching mode (ν_{OD}), the $\nu_{C=O}$ (see Supporting Information section), ν_aSO_3 and ν_sSO_3 corresponding to the AOT surfactant in the mixed RMs and the P=O stretching frequency ($\nu_{P=O}$) of TOPO in the water/TOPO/n-heptane system (see Supporting Information section). It must be pointed out that the $\nu_{P=O}$ of TOPO cannot be monitored in the mixed RMs since it appears in the same region as the very intense AOT ν_aSO_3 stretching band.

Water O-D stretching mode (ν_{OD}).

By FT-IR different kind of information can be obtained:⁶¹⁻⁶³ i) H-bond interactions between water and surfactant polar head group, including its counterion; ii) surfactant–counterion interactions, iii) different kinds of water structure solubilized in the mixed RMs media such as interfacial bound water and/or “bulk-like” water.⁶² In this case, layers of different structures, *if present*, should be detected by FT-IR spectroscopy because the time scale of this technique (10^{-12} - 10^{-14} s) is faster than the time scale on which water molecules are expected to interchange with each other (between 10^{-7} and 10^{-11} s).^{62,86} Conclusions

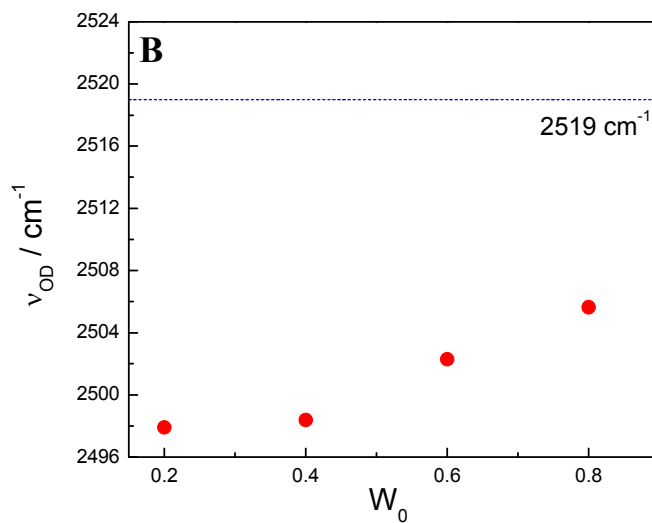
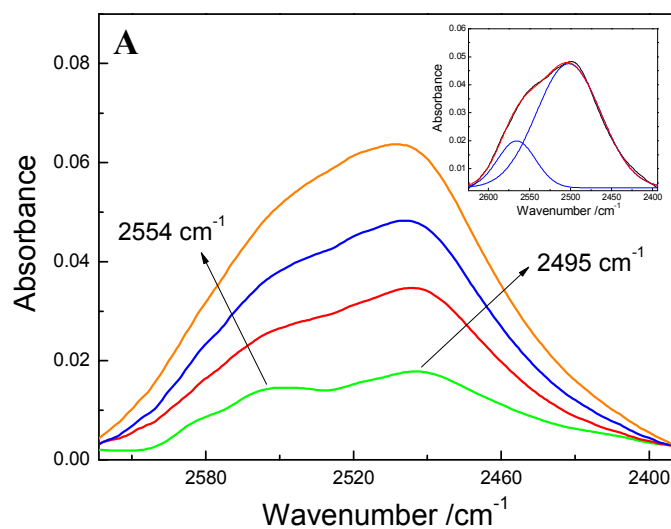
with regard to the different types of water structure entrapped inside AOT RMs are usually arrived from the number of peaks obtained by curve fitting, *e.g.*, of the ν_{OH} (from entrapped H_2O)^{34,71} and ν_{OD} (from entrapped D_2O). However, the basic premise involved in this assumption, *i.e.*, that each band obtained by curve fitting may be attributed to a different type of water, is open to question because these bands possibly originate from coupled water molecule vibrations and from a bending overtone often reported in the spectrum of liquid water.⁶¹⁻⁶³

On the other hand, deconvolution of ν_{OD} vibration of HOD is straightforward because both frequencies are essentially decoupled, provided $\text{D}_2\text{O} < 10\%$.⁶¹⁻⁶³ Moreover, the use of HOD as probe has the distinct advantage that the frequency of this band is in the region relatively free from other strong absorption.⁶³

In order to present our results in a clear manner, we introduce first the results in the RMs media with $X_{\text{TOPO}} = 1$. Figure 3A shows the FT-IR spectra in the region corresponding to the O-D stretching band (ν_{OD}) of HOD in water/TOPO/*n*-heptane system at different W_0 values. Figures 3B and C show the ν_{OD} values as a function of the water content for the same system after deconvolution of the band with two peaks.

As can be seen, at any W_0 value investigated, the O-D band present a marked asymmetry, especially at low water content, where it can be observed a main peak around 2495 cm^{-1} with a shoulder at approximately 2554 cm^{-1} . The main peak shifts to higher frequencies (2495 cm^{-1} at $W_0 = 0.2$ and 2507 cm^{-1} at $W_0 = 0.8$) with increasing the W_0 value (Figure 3B). The asymmetry of the O-D band suggests the coexistence of two different populations of water with different structure inside TOPO RMs.

For TOPO RMs we assign the main peak to water molecules strongly interacting with each other forming dimers, trimers and aggregates to higher order (“bulk-like” water) which tends to the frequency of the bulk HOD (2519 cm^{-1})⁸⁷ as W_0 values increase. On the



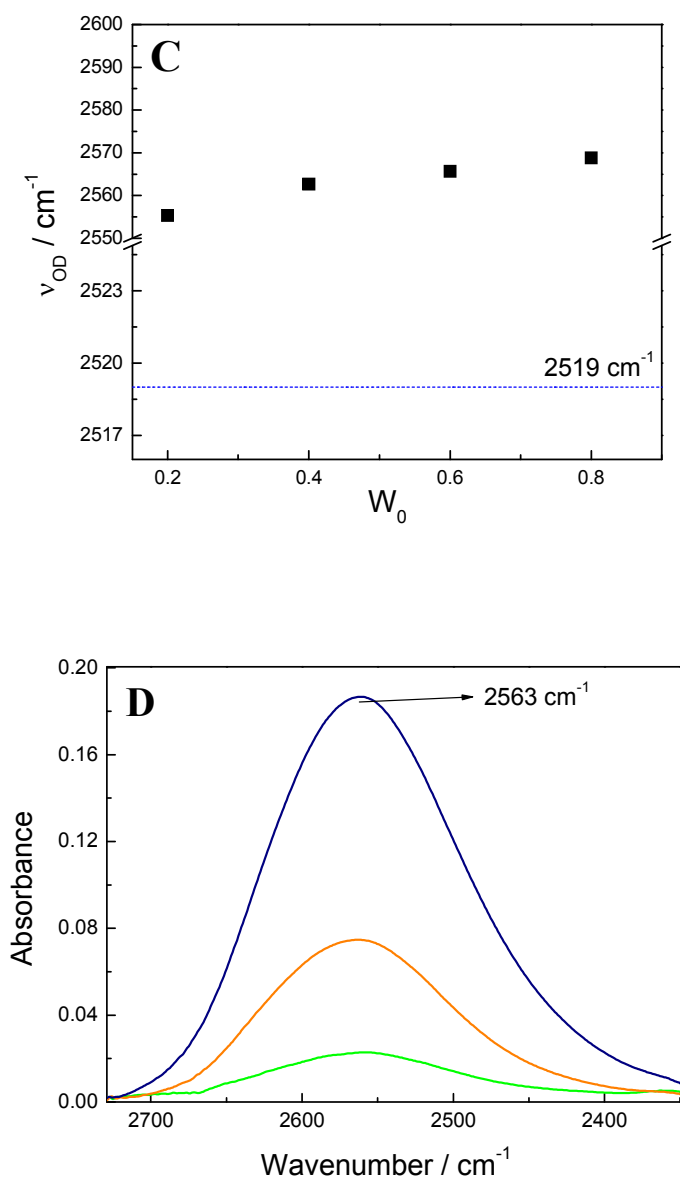


Figure 3: **A:** FT-IR spectra in the region of O-D stretching frequency (ν_{OD}) of HOD in water/TOPO/*n*-heptane reverse micelle upon increasing the W_0 values: 0.2 (—), 0.4 (—), 0.6 (—), 0.8 (—). Deconvolution of the O-D band at $W_0 = 0.6$ is shown in the inset. The black curve is the experimental one, red curve is the overall fitted curve and the blue curves are the deconvoluted curves. **B:** Shift of ν_{OD} corresponding to “bulk-like” water upon increasing the W_0 . **C:** Shift of ν_{OD} corresponding to bound water upon increasing the W_0 .

The ν_{OD} value for pure HOD (---) is included for comparison.⁸⁷ [TOPO] = 0.2 M. **D**: FT-IR spectra corresponding to the O-D stretching frequency (ν_{OD}) of HOD in water/AOT/*n*-heptane reverse micelle at $W_0 = 0.2$ (—), 0.8 (—) and 2 (—). The *n*-heptane bands have been subtracted. [AOT] = 0.2 M.

other hand, the shoulder located at 2554 cm^{-1} ($W_0 = 0.2$) corresponds to the water interacting with the TOPO polar head (bound water) through H-bond and breaking its bulk structure. Figure 3C shows that the maximum band frequency (around 2554 cm^{-1} at any W_0) is larger than the corresponding to bulk water showing that the water–TOPO interaction is still present. Furthermore, the ratio of the intensity of the band at 2495 cm^{-1} (“bulk-like” water) respect to the shoulder at 2554 cm^{-1} (bound water) increases with increasing the W_0 value. This may indicate that there is an increase in the “bulk-like” type of water at the expense of the bound water, probably because the interaction between water molecules is stronger than the water–TOPO interaction.

On the other hand, it is interesting to investigate the P=O stretching region (see Supporting Information section, Figures S1 and S2) where the following conclusions were arrived: i) water effectively interacts by H-bond with the P=O group of TOPO located at the polar side of the RMs interface and ii) TOPO molecules at the nonpolar part of the interface do not interact with water molecules.

In summary, we show that the ν_{OD} of the “bulk-like” water differs markedly from the ν_{OD} of pure water and, this could mean that the interaction between water molecules in the water/TOPO/*n*-heptane system is stronger than the one found in pure water. As in the literature there are no reports about studies of the ν_{OD} band on the AOT/*n*-heptane RMs in

the W_0 range values that TOPO forms RMs, we decided to perform the experiments in AOT/*n*-heptane RMs at the same W_0 values used for TOPO, for comparison. It must be noted that in the literature different studies about the water structure in AOT RMs using the deconvolution of the ν_{OH} vibration of water can be found but for us, the conclusions are debatable since this band is completely asymmetric as it was explained above.⁸⁸

Figure 3D shows the FT-IR spectra in the region corresponding to ν_{OD} for the water/AOT/*n*-heptane system at three W_0 values: 0.2, 0.8 and 2. The Figure also shows that the ν_{OD} is centered around 2563 cm^{-1} , which does not change its position at least in the W_0 range evaluated. Thus, for such W_0 values the structure of the encapsulated water in AOT RMs has its H-bond network broken because the interaction with the polar heads and the counterions of AOT, as it is already known.⁹⁰⁻⁹³ As it can be seen, the behavior of water inside AOT RMs is different from water confined in the TOPO/*n*-heptane system (Figure 3A). For HOD entrapped in AOT/*n*-heptane RMs a symmetric band was observed and attributed to only one kind of water present in the AOT RMs system that is, water interacting with the AOT polar head group (bound water) contrary to what claimed by Onori et al.⁸⁸

In the case of water/AOT:TOPO/*n*-heptane RMs, the water FT-IR spectra depend on the TOPO composition at W_0 value constant. Figures 4 show the FT-IR spectra in the region corresponding to the ν_{OD} for water encapsulated inside mixed RMs for different X_{TOPO} at two different W_0 values: (A) $W_0 = 0.5$ and (B) $W_0 = 2$, respectively. It should be noted that in Figure 4B the FT-IR spectrum at $X_{TOPO} = 1$ was not displayed since TOPO does not form RMs at $W_0 = 2$ (see Figure 1).

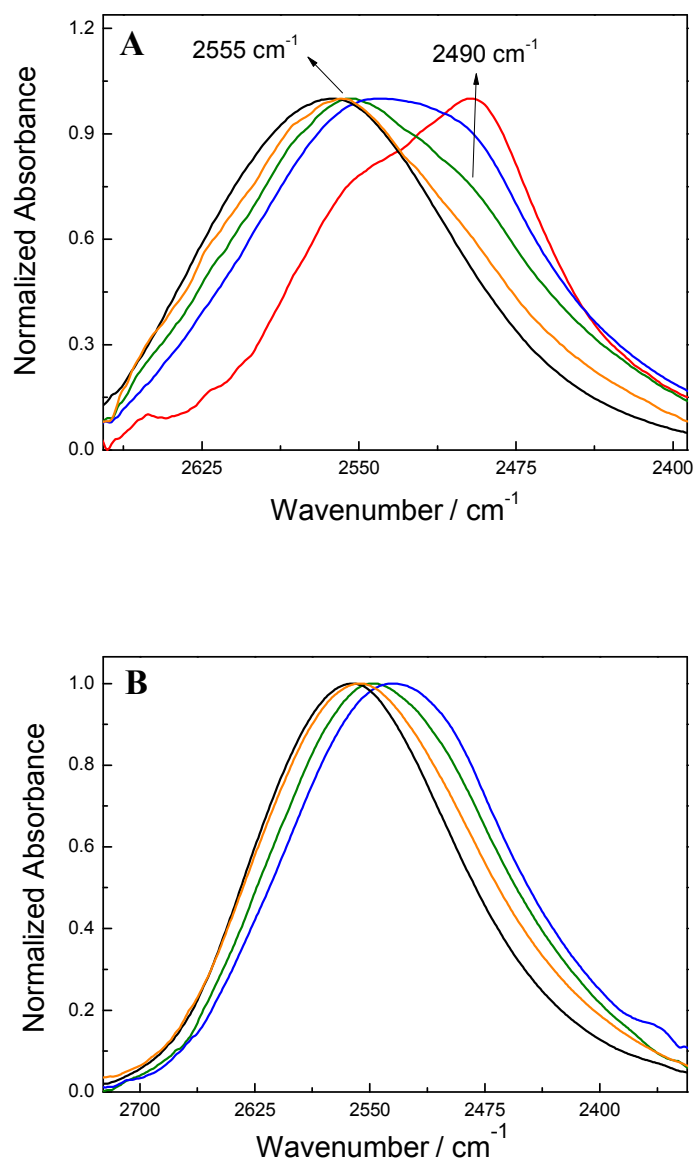


Figure 4: FT-IR spectra corresponding to the O-D stretching band of HOD in water/AOT:TOPO/*n*-heptane mixed reverse micelles upon increasing the X_{TOPO} at (A) $W_0 = 0.5$ and (B) $W_0 = 2$. $X_{\text{TOPO}} = 0$ (—), 0.3 (—), 0.5 (—), 0.7 (—), 1 (—). $[\text{Surf.}]_{\text{T}} = 0.2 \text{ M}$.

Firstly, it can be seen in Figure 4A that at low water content, the O-D band start to lose its symmetry at $X_{\text{TOPO}} \geq 0.3$ (orange line), compared to the band observed when water

is inside AOT RMs (black line). When $X_{\text{TOPO}} = 0.5$, a major peak is clearly distinguishable at 2555 cm^{-1} (bound water) with a shoulder around 2490 cm^{-1} (“bulk-like” water). In the system with $X_{\text{TOPO}} = 0.7$, the intensity of the shoulder increases and it is almost equal to the intensity of the main peak. Finally, the system formed only by TOPO shows a reversal in the relative intensities of both peaks, being now the main peak the one at 2490 cm^{-1} as it was discussed. Thus, at $W_0 = 0.5$, the presence of TOPO in the RMs alters the nature of the encapsulated water probably due to the differences in the surfactant compositions at the RM interface level. Thus, certain fraction of the water molecules seems to interact simultaneously with one or both surfactants ($\nu_{\text{OD}} = 2555 \text{ cm}^{-1}$, bound water), whereas the other fraction of the water molecules strongly interacts with each other ($\nu_{\text{OD}} \sim 2490 \text{ cm}^{-1}$, “bulk-like” water) forming a free water state, even at low water content. For example, comparing the ν_{OD} of the main peak when $X_{\text{TOPO}} = 0.5$ (Figure 4A) with the ν_{OD} of water encapsulated in TOPO RMs (Figure 3 C) can be seen a great similarity in their frequencies values: 2555 cm^{-1} and 2554 cm^{-1} respectively. Therefore, we believe that water has preferential interaction with TOPO when the water content is small probably because the RMs interface is rich in TOPO molecules as it was discussed in the DLS section.

Therefore, the high TOPO presence at the interface might be the responsible of the existence of two different kinds of water: interacting with the polar heads as well as with other water molecules. Precisely, what is unexpected for the micellar system is the existence of free water at this low values of W_0 value,⁹⁰⁻⁹³ which would not be expected in micellar systems formed mainly or with large percentage of AOT molecules at the interface.

When water is encapsulated in AOT/isooctane RMs, the H-bond interaction with the AOT polar headgroup increases the surfactants' a_0 values with the consequent decrease in the P_c , and the increase in the RMs droplet size.⁸⁹ We have recently^{9,68} shown using DLS that, besides water, in non-aqueous AOT/*n*-heptane RMs the polar solvents–AOT interactions especially the H-bond, are the key for the RMs droplets sizes control. Thus, we suspected that the unique properties of the encapsulated water in the mixed RMs systems, could also be involved in controlling the size of the mixed RMs, since differences in d_{app} compared with AOT RMs occur at $W_0 = 0.5$. Thus, as demonstrated above, the increase in the TOPO content in the mixture causes an increase in the fraction of free water molecules, at the expense of a proportional decrease in the fraction of bound water molecules. This can be explained considering that the water–TOPO interaction is weaker compared to the water–AOT interaction. Also the v_{OD} is higher in AOT RMs than TOPO RMs which suggests a more broken H-bond network in the former system (see Figure 3A and 3D). Therefore, the progressive separation of the water molecules from the interface to establish stronger interactions with each other causes the decreases in the a_{eff} and the increases in the P_{eff} and the consequent decrease in the size of the mixed aggregates when the interface is rich in TOPO. As seen in Figures 2A and B TOPO RMs are always smaller than AOT RMs, which may suggest that the TOPO's a_0 is not affected practically with the water addition because the water–TOPO interaction seems to be weaker than water–AOT one. Since a_0 for TOPO is smaller than for AOT the encapsulated water could present some preferential interaction for AOT than TOPO but, as the interface is rich in TOPO molecules, the droplet size diminishes with the TOPO content. Probably, not only the interaction of water with surfactant is affected by the presence of the nonionic surfactant,

but the interaction between water–water molecules is different in comparison with that established for the RMs formed only with AOT, where water at low values of W_0 interact strongly with the SO_3^- group.⁹⁰⁻⁹³

On the contrary, at $W_0 = 2$ (Figure 4 B) it can be seen that the profile for all the bands are completely symmetrical which means that only one kind of water is present. Increasing X_{TOPO} only causes a decrease in the ν_{OD} band as it is plotted in Figure S3 in the Supporting Information section. When the system is formed only by AOT, the $\nu_{\text{OD}} = 2563 \text{ cm}^{-1}$ and decreases to 2536 cm^{-1} when $X_{\text{TOPO}} = 0.7$. As it can be seen, increasing X_{TOPO} , causes the ν_{OD} gradually approach to the value corresponding to the ν_{OD} of the bulk water (2519 cm^{-1})⁸⁷ but does not reach it. This indicates that the properties of water encapsulated in the mixed RMs do not resemble the one of the bulk water.^{9,94} Hence, the symmetrical profiles of the bands observed in Figure 4B reflects preferentially bound water with the anionic surfactant AOT and Na^+ counterions in the interface. Furthermore, as the X_{TOPO} content increases, the presence of TOPO molecules at the interface weaken the water–AOT interaction and the O-D band shifts to lower frequencies as the X_{TOPO} content increases.

The similarity in the profiles of the bands at $W_0 = 2$ with the one obtained for the system only formed with AOT molecules (see Figure 3D) supports the results obtained by DLS, where it was suspected that the mixed interface could be made largely with AOT molecules which strongly interact with water and the RMs droplet sizes are practically independent on the TOPO content.

AOT's Groups Stretching Regions

Asymmetric S=O Stretching Band ($\nu_a\text{SO}_3$)

It is known that the $\nu_a\text{SO}_3$ bands in aqueous AOT RMs present a splitting of two intense peaks (defined as $\Delta\nu_a$) which is due to the degeneracy of these vibrations by a non symmetrical interaction of Na^+ with the SO_3^- group.⁹⁵ Also, it was shown that the magnitude of $\Delta\nu_a$ decreases with increasing micelle hydration due to a weakening of the $\text{Na}^+-\text{SO}_3^-$ interaction after H-bond interaction between water and the AOT polar head group with the corresponding increases in their spatial separation.⁹⁵ Thus, the $\Delta\nu_a$ is very useful to monitor the electrostatic interaction between Na^+ counterion and the SO_3^- group.^{95,96} Herein, we use the $\nu_a\text{SO}_3$ stretching mode to gain more insights about the kind of interactions that the water molecules sequestered by the mixed RMs have with the interface.

Figure S4 from the Supporting Information section shows the FT-IR spectra in the region of 1300-1150 cm^{-1} for water/AOT:TOPO/*n*-heptane RMs at different W_0 values at $X_{\text{TOPO}} = 0.1$ (*n*-heptane bands have been subtracted from the spectra). Similar results were obtained for the other X_{TOPO} (data not shown). As it can be seen, there is a broad profile in the frequency corresponding to the $\nu_a\text{SO}_3$ mode dominated by two strong peaks at around 1215 and 1245 cm^{-1} , for which the intensity and the $\Delta\nu_a$ depend on the water and the TOPO content. Figure 5 shows the $\Delta\nu_a$ at different W_0 values (in the 0-2 range values) and at different X_{TOPO} content (in the 0-0.7 range values).

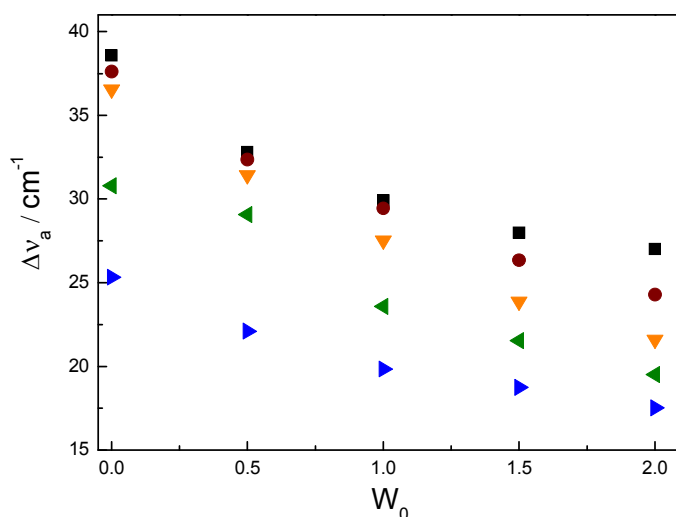


Figure 5: Splitting values of the asymmetric sulfonate stretching frequency (Δv_a) of AOT upon increasing the W_0 value at different X_{TOPO} in water/AOT:TOPO/*n*-heptane mixed reverse micelles. $X_{\text{TOPO}} = 0$ (■), 0.1 (●), 0.3 (▼), 0.5 (◄), 0.7 (►). $[\text{Surf.}]_{\text{T}} = 0.05 \text{ M}$.

In all cases, the magnitude of the Δv_a gradually decreases with increasing the water content. For AOT RMs (black squares) at $W_0 = 0$ the Δv_a value is 39 cm^{-1} and decreases to 27 cm^{-1} for $W_0 = 2$.

Focusing the analysis on the effect of the change in the X_{TOPO} in the absence of water (the y axes), the $\Delta v_a = 39 \text{ cm}^{-1}$ for $X_{\text{TOPO}} = 0$ progressively decreases up to the value of 25 cm^{-1} when the $X_{\text{TOPO}} = 0.7$. Also, the Δv_a value does not change significantly when X_{TOPO} modified from 0 to 0.3. However, there is a significant drop in its value at an equimolar ratio between the two surfactants.

The Δv_a value for mixed RMs in the absence of water when the $X_{\text{TOPO}} = 0.7$ is relatively lower than that recorded for AOT RMs in the maximum W_0 analyzed. The Δv_a

value obtained at $W_0 = 2$ is practically the same that one obtained at W_0 larger than 30.⁹⁵ This suggests that TOPO has a large affinity for the Na^+ counterions making a strong complex separating the Na^+ from the SO_3^- group in a very efficient manner. However, the most important finding is that this particular effect occurs in the absence of water. The mechanism by which the nonionic surfactant could separate the Na^+ to the polar head of AOT is based on the presence of the P=O group which can donate their free electrons pairs and so complex the cation as it is known for other metals.^{37,40}

Moreover, as can be seen in Figure 5 at $W_0 = 0.5$, the Δv_a value does not change appreciably increasing X_{TOPO} from 0 to 0.3, but starts to decrease at $X_{\text{TOPO}} = 0.5$ and it becomes even more pronounced at $X_{\text{TOPO}} = 0.7$. The same trend is observed for mixed RMs at $W_0 = 1$ and, the more remarkable changes occur at $W_0 = 2$. Something interesting to note, particularly at $W_0 = 0.5$, is the difference between the Δv_a values when $X_{\text{TOPO}} = 0.5$ and $X_{\text{TOPO}} = 0$. As can be seen from Figure 5, this difference is significantly less than that observed when the system does not contain water.

On the other hand, at $W_0 = 2$, we can see (Figure 5) that even when $X_{\text{TOPO}} = 0.1$ the TOPO content in the mixture is enough to cause a decrease in Δv_a and this decrease is proportional to the X_{TOPO} . Furthermore, the differences between the Δv_a values at $W_0 = 2$ for $X_{\text{TOPO}} = 0.5$ and the corresponding value when $X_{\text{TOPO}} = 0$ again resembles what it was observed at $W_0 = 0$. These results indicate that when the water content is low ($W_0 < 1$), the efficiency in the separation of Na^+ by TOPO is reduced for the presence of water and the separation is achieved only when the contents of TOPO in the mixture is appreciable ($X_{\text{TOPO}} \geq 0.5$). In contrast, when the water content is higher ($W_0 > 1$) TOPO recovers its

complexing capacity and with low TOPO concentrations the separation of Na^+ from the polar head of AOT is achieved.

As discussed at low W_0 values, water has a preferential interaction with TOPO because the interface of the mixed RMs is formed mainly with TOPO molecules. Hence, this interaction appears to be responsible for the diminishing of the TOPO complex power property at the interface and this would explain the low decrease in Δv_a values.

On the contrary, when the water content increases progressively in the mixed RMs, the interface becomes richer in AOT molecules and interacts more strongly with AOT than TOPO leaving free electrons pairs of the polar head of TOPO available to complex Na^+ , regenerating its complexing power. This may explain that at $W_0 > 1$ only with a low content of TOPO in the mixture ($X_{\text{TOPO}} = 0.1$) separation of Na^+ from the SO_3^- group is detected (see Figure 5).

This particular behavior, especially when the $W_0 > 1$, suggests the existence of a combined effect between TOPO and water causing two complementary actions: removal Na^+ counterions from the polar head of AOT and, simultaneously the formation of $\text{Na}^+\cdot\text{TOPO}$ complex. It may be noted that the Δv_a value of AOT RMs in absence of water is 39 cm^{-1} . In contrast, for the maximum W_0 and X_{TOPO} values analyzed in mixed RMs the $\Delta v_a = 17 \text{ cm}^{-1}$ showing a clear combined effect between TOPO and water on the Na^+ separation.

Symmetric S=O Stretching Band ($\nu_s\text{SO}_3$)

The addition of water to the RMs system, causes a shift in the $\nu_s\text{SO}_3$ to lower frequencies (from 1051 to 1045 cm^{-1} when the W_0 values increased from 0 to 20; the greatest changes were observed at $W_0 < 3$).^{91,95,97} These shifts have been attributed to H-

bond interactions between the water molecules and the SO_3^- group of AOT. Also, the H-bond weakens the electrostatic cation–anion interactions, which are also affected by charge–dipole interactions between water and the sodium counterion.

Figure S5 from the Supporting Information section, shows the FT-IR spectra of the $\nu_s\text{SO}_3$ mode increasing the X_{TOPO} at $W_0 = 0$. Figures S6 A and B from the Supporting Information section show the FT-IR band spectra of the $\nu_s\text{SO}_3$ mode at different water content for $X_{\text{TOPO}} = 0.1$ and 0.7 respectively. Figure 6 shows the shifting of the $\nu_s\text{SO}_3$ for AOT upon increasing the W_0 at different X_{TOPO} values in mixed RMs. Firstly, without water addition, it can be seen a noticeable decreases of the $\nu_s\text{SO}_3$ upon addition of TOPO. For example, it changes from 1052 cm^{-1} for $X_{\text{TOPO}} = 0$ to 1044 cm^{-1} for $X_{\text{TOPO}} = 0.7$. On the other hand, and analyzing the water effect it can be observed that for $X_{\text{TOPO}} = 0$, the $\nu_s\text{SO}_3$ decreases from 1052 cm^{-1} for $W_0 = 0$, to 1050 cm^{-1} for $W_0 = 2$.

It is important to note and to compare the $\nu_s\text{SO}_3$ values obtained at the extreme points of the systems discussed above. That is, in the AOT RMs at the maximum W_0 value analyzed ($X_{\text{TOPO}} = 0$, $W_0 = 2$) and the mixed RMs in the absence of water ($X_{\text{TOPO}} = 0.7$, $W_0 = 0$). As it can be seen, increasing the water content in the AOT RMs leads to a reduction of about 2 cm^{-1} in the frequency, while increasing the TOPO content in the absence of water, causes a reduction in the frequency of $\sim 8\text{ cm}^{-1}$. That is, the nonionic surfactant complexes the Na^+ counterion resulting in the weakening of the $\text{Na}^+ - \text{SO}_3^-$ interaction more efficiently

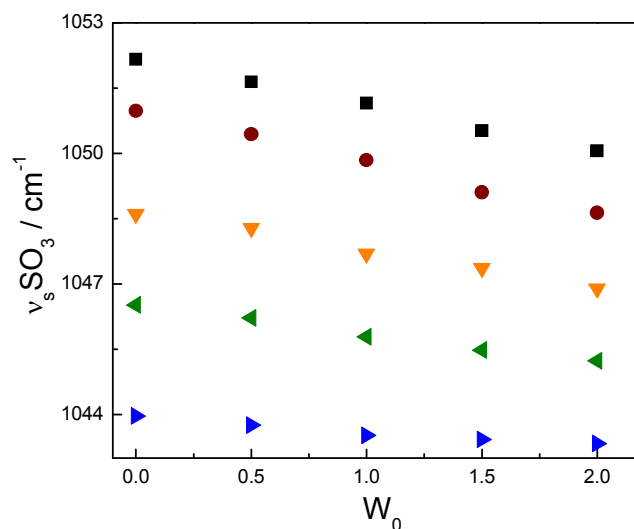


Figure 6: Shift of the symmetric sulfonate stretching frequency ($\nu_s\text{SO}_3$) of AOT upon increasing the W_0 at different X_{TOPO} values in water/AOT:TOPO/*n*-heptane mixed reverse micelles. $X_{\text{TOPO}} = 0$ (■), 0.1 (●), 0.3 (▼), 0.5 (◄), 0.7 (►). [Surf.]T = 0.05 M.

than water. This affirmation can be corroborated as follow, for example, for $X_{\text{TOPO}} = 0.1$ (see Figure 6) there is a decrease of the $\nu_s\text{SO}_3$ when the water content increases which is similar to the one observed at $X_{\text{TOPO}} = 0$. However, when the $X_{\text{TOPO}} = 0.7$, increasing the W_0 value there is little change of the $\nu_s\text{SO}_3$. These results indicate that when the X_{TOPO} is low, TOPO at the interface has not influence in the weakening of the $\text{Na}^+ - \text{SO}_3^-$ interaction and water is the molecule that really weakens this interaction. By contrast, when the X_{TOPO} content is high, the large numbers of TOPO molecules at the interface effectively separate the Na^+ counterion from the SO_3^- group. Consequently, increasing the water content has little effect because the $\text{Na}^+ - \text{SO}_3^-$ interaction is already weakened. These results are consistent with those observed in the case of asymmetric stretching mode.

Carbonyl Stretching Band ($\nu_{C=O}$)

In the Supporting Information section it can be found the study performed on the carbonyl stretching band of AOT in presence of TOPO. Figures S7, S8 and Scheme S1 show that because TOPO makes strong complex with the Na^+ counterions separating it from the AOT SO_3^- group, the C=O band is considerably more symmetric. These results suggest that the interaction between Na^+ and SO_3^- group may have impact in the asymmetry of the C=O band contrary to what it was claimed in the literature.^{82,85,96}

CONCLUSION

In this work we have shown the existence of two different and novel RMs media, one formed only with the nonionic surfactant TOPO, water/TOPO/*n*-heptane, and others made with the mix of TOPO and AOT to give water/AOT:TOPO/*n*-heptane mixed RMs.

DLS experiments shows the existence of discrete droplets at any W_0 values investigated and, in contrast what was obtained when other nonionic surfactants are mixed with AOT, the droplets sizes diminishes with the TOPO content and the changes in the droplets sizes depends on the water content; at $W_0 = 0.5$ the droplet sizes diminished significantly upon increasing the TOPO content while, at $W_0 = 2$ the changes are almost negligible and the sizes of the mixed RMs at different X_{TOPO} do not differ substantially compared to size of AOT RMs. Thus, we believe that when the water content is around $W_0 = 0.5$, the percentage of TOPO molecules at the mixed RMs interface is higher than the corresponding to the prepared solution. This is equivalent to an increase in the mole fraction of TOPO at the interface (x_{TOPO}), which results on the increment in the P_{eff} value

and, the consequent decreased in size. On the other hand, at $W_0 = 2$ we suggest that the micellar interface has more AOT molecules.

With regard to the water structure, we showed unexpected results. For example, for water/TOPO/*n*-heptane RMs the FT-IR data show the existence of two different kind of water that coexist in the RMs media, one bound to TOPO through H-bond and other strongly associated with other water molecules, the “bulk-like” structure, even at very low water content. For mixed RMs the water structure depend on the W_0 values, in this way, at $W_0 = 0.5$ when the mixed RMs are comprised mainly with TOPO molecules, there are two kinds of water molecules while for $W_0 = 2$ there is only one kind of water, the bound to the AOT through H-bond interaction.

Those differences in both the water structure as well as in the RMs interfacial composition have dramatic changes in the formation of the $\text{Na}^+\cdot\text{TOPO}$ complex. Thus, when $W_0 < 1$ the complex power diminishes because the P=O group is involved in H-bond interaction with water. At higher water content because water is involved in the interaction with AOT, there is a combined effect between the TOPO and water causing two complementary actions: removal of Na^+ counterions from the polar head of AOT and, simultaneous the formation of $\text{Na}^+\cdot\text{TOPO}$ complex.

We anticipate that the fact that free water can be found at very low water content and the complex properties of TOPO is enhanced in the mixed RMs are exciting and very encouraging results to use these novel mixed RMs as nanoreactor for different kind of reaction and nanoparticles synthesis.

ACKNOWLEDGMENTS

We gratefully acknowledge the financial support for this work by the Consejo Nacional de Investigaciones Científicas y Técnicas (CONICET), Agencia Córdoba Ciencia, Agencia Nacional de Promoción Científica y Técnica and Secretaría de Ciencia y Técnica de la Universidad Nacional de Río Cuarto. N.M.C., J.J.S. and R.D.F. hold a research position at CONICET. E.O. thanks CONICET for a research fellowship.

SUPPORTING INFORMATION AVAILABLE

Figure S1: FT-IR spectra corresponding to the phosphoryl group stretching band of TOPO in TOPO/*n*-heptane (—), TOPO/CCl₄ (—) at $W_0 = 0$ and solid TOPO (—); Figure S2: (A) FT-IR spectra corresponding to the phosphoryl group stretching band of TOPO in water/TOPO/*n*-heptane reverse micelles upon increasing the W_0 value. W_0 : 0 (—), 0.2 (—), 0.25 (—), 0.4 (—), 0.5 (—), 0.6 (—), 0.8 (—). (B) Shift of the phosphoryl group stretching frequency ($\nu_{P=O}$) of TOPO in water/TOPO/*n*-heptane reverse micelles upon increase the W_0 value; Figure S3: Shift of O-D stretching frequency (ν_{OD}) for HOD upon increasing the X_{TOPO} in water/AOT:TOPO/*n*-heptane mixed reverse micelles at $W_0 = 2$. The ν_{OD} value for pure HOD (---) is included for comparison.⁹⁸ [Surf.]_T = 0.2 M; Figure S4: FT-IR spectra in the region of 1100-1300 cm⁻¹ for AOT upon increasing the W_0 value at $X_{TOPO} = 0.1$ in water/AOT:TOPO/*n*-heptane mixed reverse micelles. W_0 : 0 (—), 0.5 (—), 1.0 (—), 1.5 (—), 2.0 (—); Figure S5: Normalized FT-IR spectra corresponding to the symmetric sulfonate stretching band of AOT upon increasing the X_{TOPO} at $W_0 = 0$ in AOT:TOPO/*n*-heptane mixed reverse micelles. X_{TOPO} : 0 (—), 0.1 (—), 0.3 (—), 0.5 (—), 0.7 (—). [Surf.]_T = 0.05 M; Figure S6: FT-IR spectra corresponding to the symmetric sulfonate stretching mode of AOT upon increasing the W_0 value at (A) $X_{TOPO}=0.1$ and (B) $X_{TOPO}=0.7$ in

water/AOT:TOPO/*n*-heptane mixed reverse micelles. W_0 : 0 (—), 0.5 (—), 1.0 (—), 1.5 (—), 2.0 (—); Figure S7: FT-IR spectra corresponding to the carbonyl stretching mode of AOT upon increasing the W_0 value at $X_{\text{TOPO}}=0.7$ in water/AOT:TOPO/*n*-heptane mixed reverse micelles. W_0 : 0 (—), 0.5 (—), 1.0 (—), 1.5 (—), 2.0 (—); Figure S8: FT-IR spectra of AOT:TOPO/*n*-heptane mixed reverse micelles at $W_0 = 0$, in the region of 1800 - 1600 cm^{-1} ($\nu_{\text{C=O}}$). X_{TOPO} : 0 (—), 0.1 (—), 0.3 (—), 0.5 (—), 0.7 (—). $[\text{Surf.}]_{\text{T}} = 0.05 \text{ M}$; Scheme S1: preferred rotational conformers of AOT in reverse micelles.

REFERENCES

- 1- S. P. Moulik and B. K. Paul, *Adv. Colloid Interface Sci.*, 1998, **78**, 99.
- 2- J. J. Silber, A. Biasutti, E. Abuin and E. Lissi, *Adv. Colloid Interface Sci.*, 1999, **82**, 189.
- 3- T. K. De and A. Maitra, *Adv. Colloid Interface Sci.*, 1995, **59**, 95.
- 4- J. Gu and Z. A. Schelly, *Langmuir*, 1997, **13**, 4256.
- 5- D. Mandal, A. Datta and S. K. Pal, K. Bhattacharyya, *J. Phys. Chem. B*, 1998, **102**, 9070.
- 6- R. McNeil and J. K. Thomas, *J. Colloid Interface Sci.*, 1981, **83**, 57.
- 7- A. Jada, J. Lang and R. Zana, *J. Phys. Chem.*, 1990, **94**, 381.
- 8- A. Jada, J. Lang, R. Zana, R. Makhoulfi, E. Hirsch and S. J. Candau, *J. Phys. Chem.*, 1990, **94**, 387.
- 9- N. M. Correa, M. A. Biasutti and J. J. Silber, *J. Colloid Interface Sci.*, 1995, **172**, 71.
- 10- N. M. Correa and N. E. Levinger, *J. Phys. Chem. B* 2006, **110**, 13050.
- 11- D. Grand and A. Dokutchaev, *J. Phys. Chem. B.*, 1997, **101**, 3181.

- 12- P. D. I. Fletcher, A. M. Howe and B. H. Robinson, *J. Chem. Soc., Faraday Trans.1*, 1987, **83**, 985.
- 13- Melo, E. P.; Aires-Barros, M. R.; Cabral, J. M. S., Reverse micelles and protein biotechnology. In *Biotechnology Annual Review*, Elsevier: 2001; Vol. Volume 7, pp 87
- 14- N. Streitner, C. Voß and E. Flaschel, *J. Biotechnol.*, 2007, **131**, 188.
- 15- Furusaki, S.; Ichikawa, S.; Goto, M., Recent advances in reversed micellar techniques for bioseparation. In *Prog. Biotechnol.*, I. Endo, T. N. S. K.; Yonemoto, T., Eds. Elsevier: 2000; Vol. Volume 16, pp 133.
- 16- D. Chen and M. Liao, *J. Mol. Catal. B: Enzym.*, 2002, **18**, 155.
- 17- A. Shome, S. Roy and P. K. Das, *Langmuir*, 2007, **23**, 4130.
- 18- A. K. Poulsen, L. Arleth, K. Almdal and A. M. Scharff-Poulsen, *J. Colloid Interface Sci.*, 2007, **306**, 143.
- 19- J. Zhang, B. Han, J. Liu, X. Zhang, J. He, Z. Liu, T. Jiang and G. Yang, *Chem. Eur. J.*, 2002, **8**, 3879.
- 20- D. Liu, J. Ma, H. Cheng and Z. Zhao, *Colloids Surf. A*, 1998, **143**, 59.
- 21- R. K. Mitra and B. K. Paul, *Colloids Surf. A*, 2005, **255**, 165.
- 22- B. K Paul and R. K Mitra, *J. Colloid Interface Sci.*, 2005, **288**, 261.
- 23- T. Kinugasa, A. Kondo, S. Nishimura, Y. Miyauchi, Y. Nishii, K. Watanabe and H. Takeuchi, *Colloids Surf. A*, 2002, **204**, 193.
- 24- D. Liu, J. Ma, H. Cheng and Z. Zhao, *Colloids Surf. A*, 1998, **139**, 21.
- 25- S. Chatterjee, R. K. Mitra, B. K. Paul and S. C. Bhattacharya, *J. Colloid Interface Sci.*, 2006, **298**, 935.
- 26- S. Chatterjee, S. Nandi and S. C. Bhattacharya, *Colloids Surf. A*, 2006, **279**, 58.

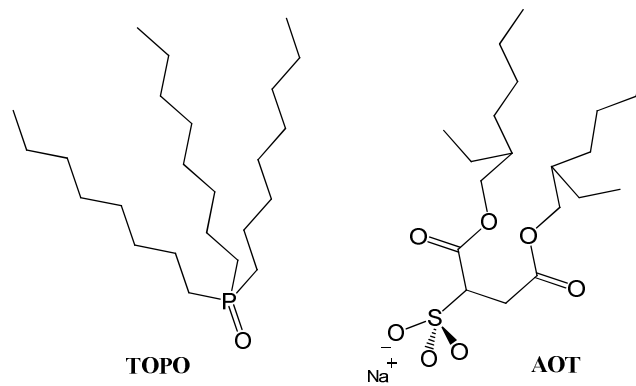
- 27- R. K. Mitra and B. K. Paul, *Colloids Surf. A*, 2005, **252**, 243.
- 28- A. Bumajdad, J. Eastoe, R. K. Heenan, J. R. Lu, D. C. Steytler and S. Egelhaaf, *J. Chem. Soc. Faraday Trans.*, 1998, **94**, 2143.
- 29- A. Bumajdad, J. Eastoe, P. Griffiths, D. C. Steytler, R. K. Heenan, J. R. Lu and P. Timmins, *Langmuir*, 1999, **15**, 5271.
- 30- A. Bumajdad, J. Eastoe, S. Nave, D. C. Steytler, R. K. Heenan and I. Grillo, *Langmuir*, 2003, **19**, 2560.
- 31- J. B. Brubach, A. Mermet, A. Filabozzi, A. Gerschel, D. Lairez, M. P. Krafft and P. Roy, *J. Phys. Chem. B.*, 2000, **105**, 430.
- 32- Q. Li, T. Li and J. Wu, *J. Phys. Chem. B*, 2000, **104**, 9011.
- 33- D. Liu, J. Ma, H. Cheng and Z. Zhao, *Colloids Surf. A*, 1998, **135**, 157.
- 34- A. Das, A. Patra and R. K. Mitra, *J. Phys. Chem. B*, 2013, **117**, 3593.
- 35- J. Kriz, J. Dybal, E. Makrlík, J. Budka and P. Vanura, *J. Phys. Chem. A*, 2009, **113**, 5896.
- 36- M. J. Schick, *Nonionic surfactants: Physical chemistry*, Dekker, New York, 1987, Vol. 23.
- 37- K. Hąc-Wydro, P. Wydro and P. Dynarowicz-Łątka, *Thin Solid Films*, 2008, **516**, 8839.
- 38- H.-X. Huang, H.-G Liu, Q.-B Xue and D.-J. Qian, *Colloids Surf. A*, 1999, **154**, 327.
- 39- Y. V. Ghalsasi and V. M. Shinde, *J. Radioanal. Nucl. Chem.*, 1998, **231**, 133.
- 40- V. K. Manchanda, K. Chander, N. P. Singh and G. M. Nair, *J. Inorg. Nucl. Chem.*, 1977, **39**, 1039.
- 41- H. Moriya and T. Sekine, *Bull. Chem. Soc. Jpn.*, 1972, **45**, 1626.

- 42- D. M. Petkovic, A. L. Ruvarac, J. M. Konstantinovic and V. K. Trujic, *J. Chem. Soc., Dalton Trans.*, 1973, **16**, 1649.
- 43- P. S. Kulkarni, *Chem. Eng. J.*, 2003, **92**, 209.
- 44- P. S. Kulkarni, S. Mukhopadhyay, M. P. Bellary and S. K. Ghosh, *Hydrometallurgy*, 2002, **64**, 49.
- 45- K. Matsumoto, Y. Tsukahara, T. Uemura, K. Tsunoda, H. Kume, S. Kawasaki, J. Tadano and T. Matsuya, *J. Chromatogr. B*, 2002, **773**, 135.
- 46- A. G. Coedo, M. T. Dorado, F. J. Alguacil and I. Padilla, *Talanta*, 1996, **43**, 313.
- 47- M. Krea and H. Khalaf, *Hydrometallurgy*, 2000, **58**, 215.
- 48- J. L. Cortina, N. Miralles, A. M. Sastre and M. Aguilar, *Hydrometallurgy*, 1995, **37**, 301.
- 49- L. Soko, L. Chimuka, E. Cukrowska and S. Pole, *Anal. Chim. Acta*, 2003, **485**, 25.
- 50- A. J. Morris-Cohen, M. T. Frederick, G. D. Lilly, E. A. McArthur and E. A. Weiss, *J. Phys. Chem. Lett.*, 2010, **1**, 1078.
- 51- M. A. López-Quintela, C. Tojo, M. C. Blanco, L. García Rio and J. R. Leis, *Curr. Opin. Colloid Interface Sci.*, 2004, **9**, 264.
- 52- A. J. Morris-Cohen, M. D. Donakowski, K. E. Knowles and E. A. Weiss, *J. Phys. Chem. C.*, 2010, **114**, 897.
- 53- C. B. Murray, D. J. Norris and M. G. Bawendi, *J. Am. Chem. Soc.*, 1993, **115**, 8706.
- 54- J. E. B. Katari, V. L. Colvin and A. P. Alivisatos, *J. Phys. Chem.*, 1994, **98**, 4109.
- 55- M. F. Galal, *J. Am. Chem. Soc.*, 1998, **120**, 5343.
- 56- L. Qu, Z. A. Peng and X. Peng, *Nano Lett.*, 2001, **1**, 333.
- 57- L. Qu and X. Peng, *J. Am. Chem. Soc.*, 2002, **124**, 2049.

- 58- L. Qu, W. W. Yu and X. Peng, *Nano Lett.*, 2004, **4**, 465.
- 59- A. Salabat, J. Eastoe, K. J. Mutch and R. F. Tabor, *J. Colloid Interface Sci.*, 2008, **318**, 244.
- 60- M. A. Sedgwick, A. M. Trujillo, N. Hendricks, N. E. Levinger and D. C. Crans, *Langmuir*, 2011, **27**, 948.
- 61- N. M. Correa, P. A. R. Pires, J. J. Silber and O. A. El Seoud, *J. Phys. Chem. B*, 2005, **109**, 21209.
- 62- O. A. El Seoud, N. M. Correa and L. P. Novaki, *Langmuir*, 2001, **17**, 1847.
- 63- L. P. Novaki, N. M. Correa, J. J. Silber and O. A. El Seoud, *Langmuir*, 2000, **16**, 5573.
- 64- M. J. Hou and D. O. Shah, *Langmuir*, 1987, **3**, 1086.
- 65- K. Kundu and B. K. Paul, *Colloids Surf. A*, 2013, **433**, 154.
- 66- R. Leung and D. O. Shah, *J. Colloid Interface Sci.*, 1987, **120**, 330.
- 67- R. Leung and D. O. Shah, *J. Colloid Interface Sci.*, 1987, **120**, 320.
- 68- R. D. Falcone, J. J. Silber, and N. M. Correa, *Phys. Chem. Chem. Phys.*, 2009, **11**, 11096.
- 69- D. F. Evans and B. W. Ninham, *J. Phys. Chem.*, 1986, **90**, 226.
- 70- C. Tanford, *J. Phys. Chem.*, 1972, **76**, 3020.
- 71- R. K. Mitra, S. S. Sinha, P. K. Verma and S. K. Pal, *J. Phys. Chem. B.*, 2008, **112**, 12946.
- 72- S. Brunetti, D. Roux, A. M. Bellocq, G. Fourche and P. Bothorel, *J. Phys. Chem.*, 1983, **87**, 1028.
- 73- F. M. Agazzi, R. D. Falcone, J. J. Silber and N. M. Correa, *J. Phys. Chem. B*, 2011, **115**, 12076.

- 74- F. M. Agazzi, J. Rodriguez, R. D. Falcone, J. J. Silber and N. M. Correa, *Langmuir*, 2013, **29**, 3556.
- 75- P. D. I. Fletcher, M. F. Galal and B. H. Robinson, *J. Chem. Soc. Faraday Trans. 1*, 1984, **80**, 3307.
- 76- R. E. Riter, E. P. Undiks, J. R. Kimmel and N. E. Levinger, *J. Phys. Chem. B.*, 1998, **102**, 7931.
- 77- R. E. Riter, J. R. Kimmel, E. P. Undiks and N. E. Levinger, *J. Phys. Chem. B.*, 1997, **101**, 8292.
- 78- Y. Gao, N. Li, L. Zheng, X. Bai, L. Yu, X. Zhao, J. Zhang, M. Zhao and Z. Li, *J. Phys. Chem. B.*, 2007, **111**, 2506.
- 79- N. M. Correa, J. J. Silber, R. E. Riter and N. E. Levinger, *Chem. Rev.*, 2012, **112**, 4569.
- 80- Q. Li, T. Li and J. Wu, *J. Colloid Interface Sci.*, 2001, **239**, 522.
- 81- S. Bardhan, K. Kundu, S. K. Saha and B. K. Paul, *J. Colloid Interface Sci.*, 2013, **411**, 152.
- 82- T. K. Jain, M. Varshney and A. Maitra, *J. Phys. Chem.*, 1989, **93**, 7409.
- 83- G. Calvaruso, A. Minore and V. T. Liveri, *J. Colloid Interface Sci.*, 2001, **243**, 227.
- 84- A. M. Durantini, R. D. Falcone, J. J. Silber and N. M. Correa, *Chem. Phys. Chem.*, 2009, **10**, 2034.
- 85- D. J. Christopher, J. Yarwood, P. S. Belton and B. P. Hills, *J. Colloid Interface Sci.*, 1992, **152**, 465.
- 86- G. E. Walrafen, *J. Chem. Phys.*, 1968, **48**, 244.
- 87- M. Falk, *J. Chem. Phys.*, 1987, **87**, 28.
- 88- G. Onori and A. Santucci, *J. Phys. Chem.*, 1993, **97**, 5430.

- 89- A. Maitra, *J. Phys. Chem.*, 1984, **88**, 5122.
- 90- M. Zulauf and H. F. Eicke, *J. Phys. Chem.*, 1979, **83**, 480.
- 91- Q. Li, S. Weng, J. Wu and N. Zhou, *J. Phys. Chem. B.*, 1998, **102**, 3168.
- 92- A. Goto, H. Yoshioka, M. Manabe and R. Goto, *Langmuir*, 1995, **11**, 4873.
- 93- S. Das, A. Datta and K. Bhattacharyya, *J. Phys. Chem. A.*, 1997, **101**, 3299.
- 94- B. Bharat, J. M. Roden, M. Sedgwick, N. M. Correa, D. C. Crans and N. E. Levinger, *J. Am. Chem. Soc.*, 2006, **128**, 12758.
- 95- P. D. Moran, G. A. Bowmaker, R. P. Cooney, J. R. Bartlett and J. L. Woolfrey, *Langmuir*, 1995, **11**, 738.
- 96 P. D. Moran, G. A. Bowmaker, R. P. Cooney, J. R. Bartlett and J. L. Woolfrey, *J. Mater. Chem.*, 1995, **5**, 295.
- 97- H. Kise, K. Iwamoto and M. Sen, *Bull. Chem. Soc. Jpn.*, 1982, **55**, 3856.
- 98- M. Falk, *J. Chem. Phys.*, 1987, **87**, 28.



Scheme 1: Molecular structure of TOPO and AOT surfactants.

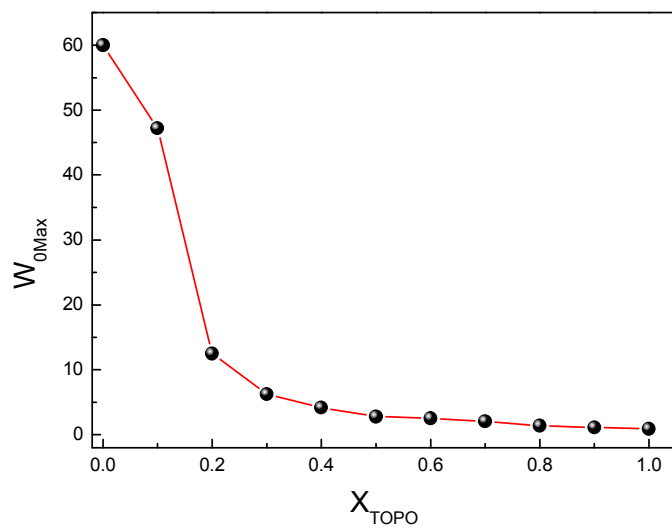


Figure 1: Maximum amount of water solubilized ($W_{0\text{Max}}$) in AOT:TOPO/*n*-heptane mixed systems as a function of X_{TOPO} . $[\text{Surf.}]_{\text{T}} = 0.2 \text{ M}$.

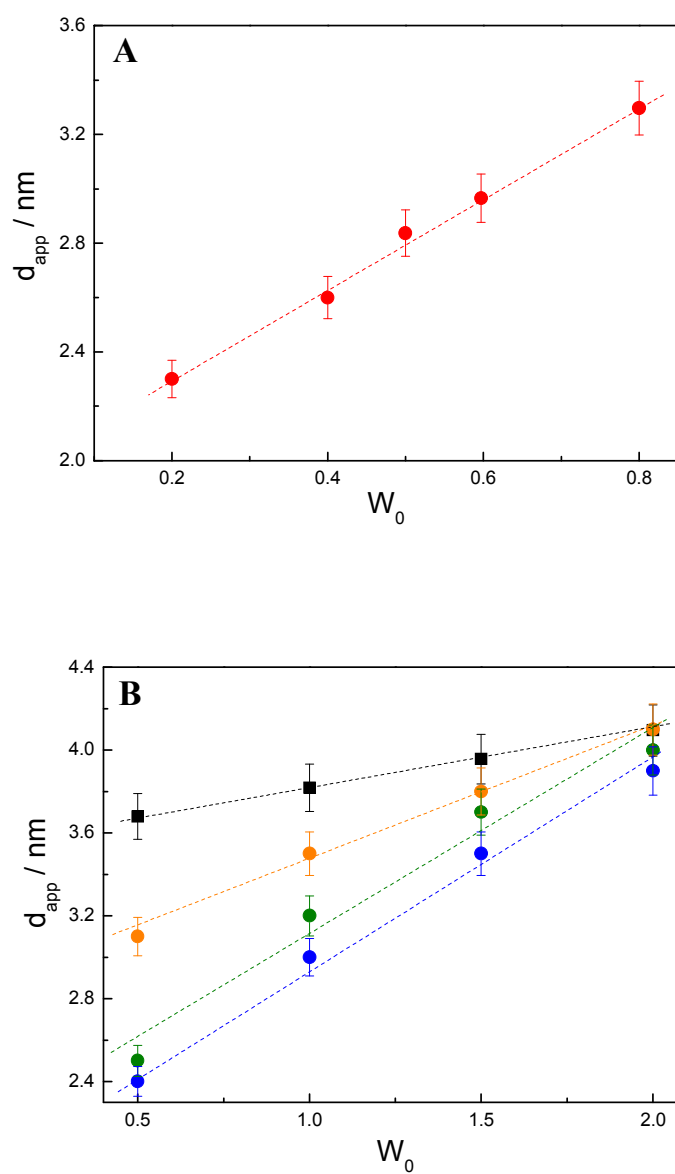
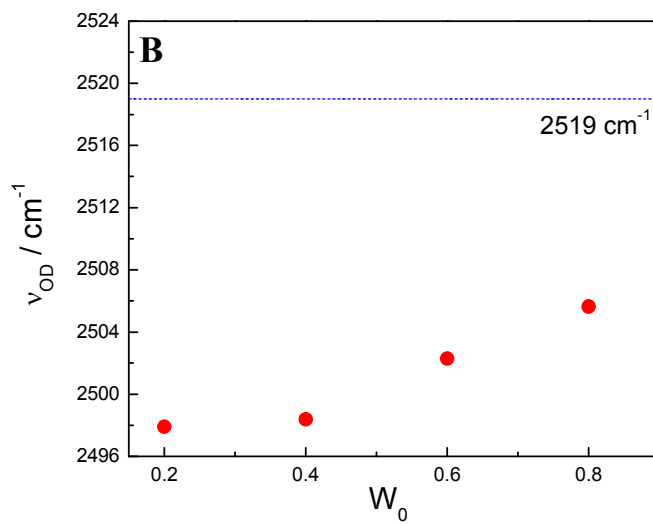
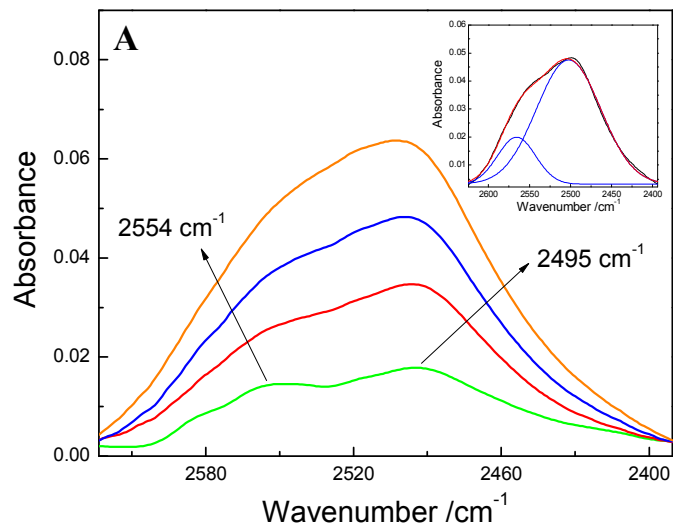


Figure 2: Water/AOT:TOPO/*n*-heptane droplets apparent diameters (d_{app}) as a function of W_0 for (A) $X_{TOPO} = 1$ and (B) $X_{TOPO} = 0$ (■) extrapolated from ref. 12, 0.3 (●), 0.5 (●) and 0.7 (●). $[\text{Surf.}]_T = 0.2$ M.



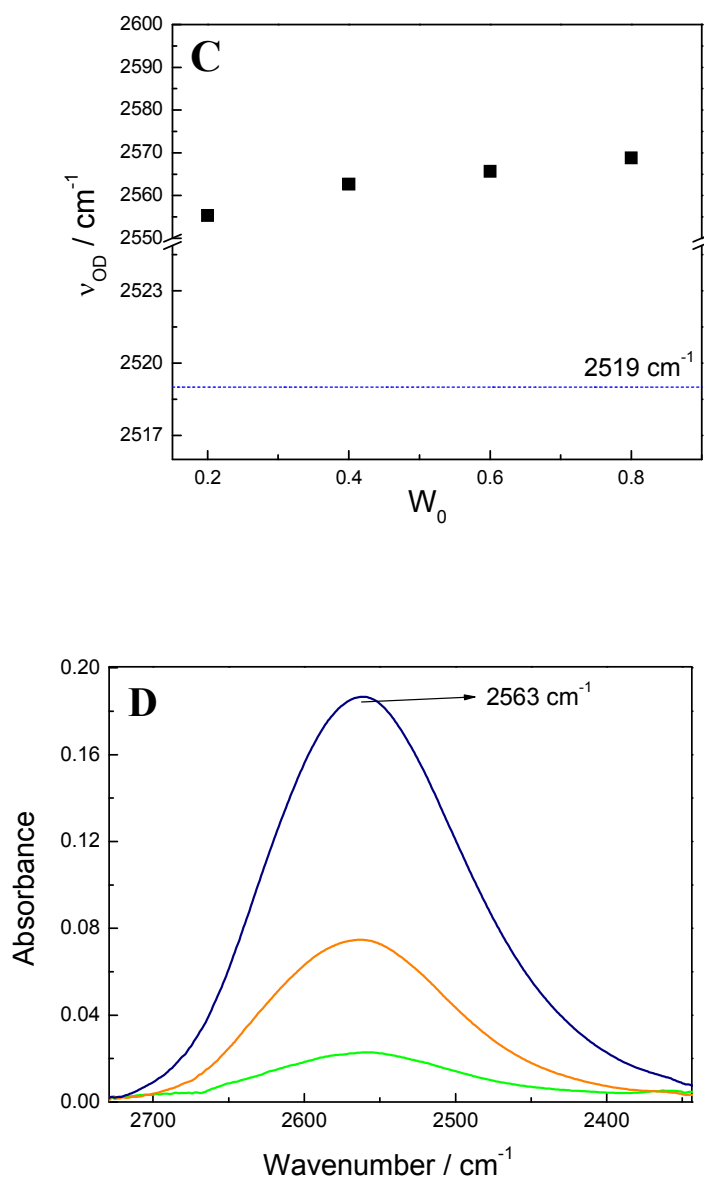


Figure 3: A: FT-IR spectra in the region of O-D stretching frequency (ν_{OD}) of HOD in water/TOPO/*n*-heptane reverse micelle upon increasing the W_0 values: 0.2 (—), 0.4 (—), 0.6 (—), 0.8 (—). Deconvolution of the O-D band at $W_0 = 0.6$ is shown in the inset. The black curve is the experimental one, red curve is the overall fitted curve and the blue curves are the deconvoluted curves. B: Shift of ν_{OD} corresponding to “bulk-like” water upon increasing the W_0 . C: Shift of ν_{OD} corresponding to bound water upon increasing the W_0 .

The ν_{OD} value for pure HOD (---) is included for comparison.⁸⁷ [TOPO] = 0.2 M. **D**: FT-IR spectra corresponding to the O-D stretching frequency (ν_{OD}) of HOD in water/AOT/*n*-heptane reverse micelle at $W_0 = 0.2$ (—), 0.8 (—) and 2 (—). The *n*-heptane bands have been subtracted. [AOT] = 0.2 M.

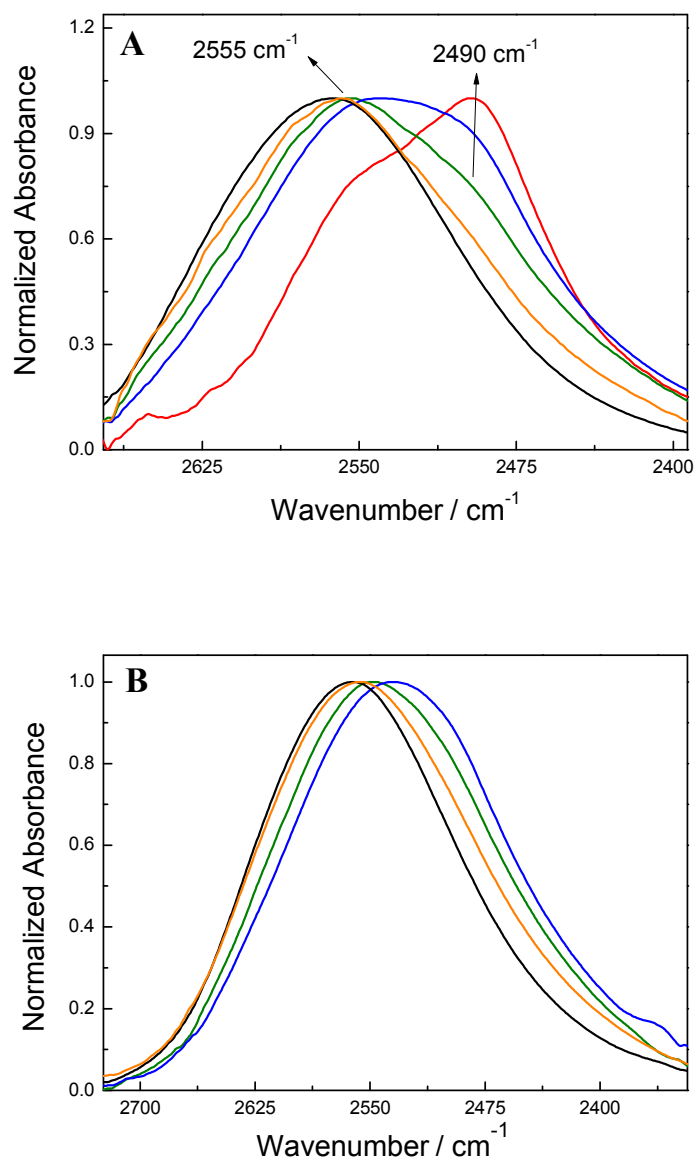


Figure 4: FT-IR spectra corresponding to the O-D stretching band of HOD in water/AOT:TOPO/*n*-heptane mixed reverse micelles upon increasing the X_{TOPO} at (A) $W_0 = 0.5$ and (B) $W_0 = 2$. $X_{\text{TOPO}} = 0$ (—), 0.3 (—), 0.5 (—), 0.7 (—), 1 (—). $[\text{Surf.}]_{\text{T}} = 0.2 \text{ M}$.

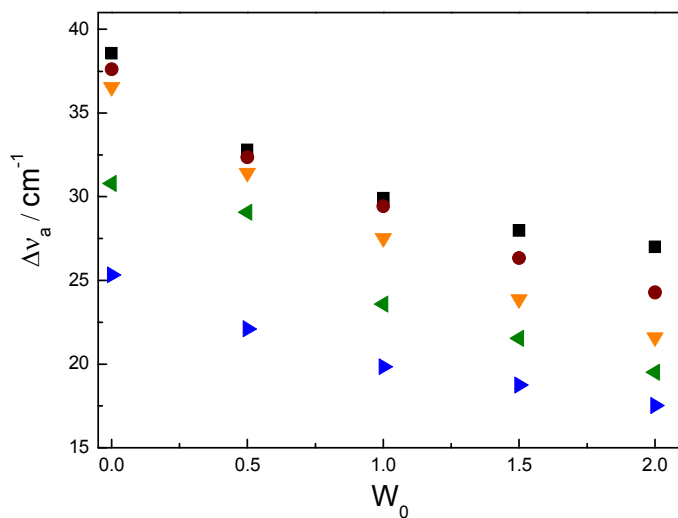


Figure 5: Splitting values of the asymmetric sulfonate stretching frequency (Δv_a) of AOT upon increasing the W_0 value at different X_{TOPO} in water/AOT:TOPO/*n*-heptane mixed reverse micelles. $X_{\text{TOPO}} = 0$ (■), 0.1 (●), 0.3 (▼), 0.5 (◄), 0.7 (►). $[\text{Surf.}]_{\text{T}} = 0.05 \text{ M}$.

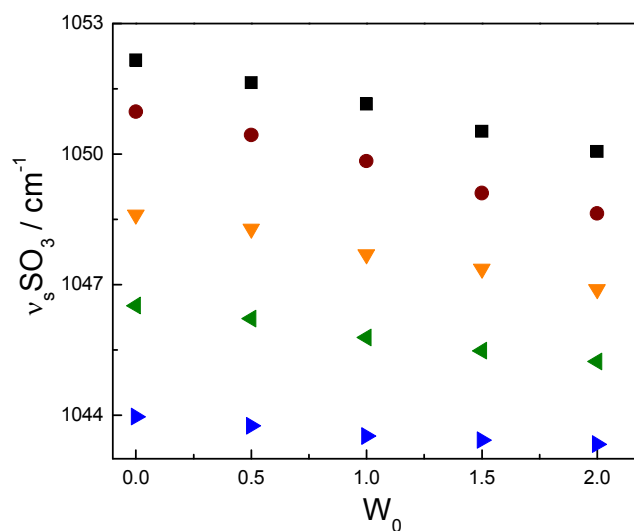


Figure 6: Shift of the symmetric sulfonate stretching frequency ($\nu_s \text{SO}_3$) of AOT upon increasing the W_0 at different X_{TOPO} values in water/AOT:TOPO/*n*-heptane mixed reverse micelles. $X_{\text{TOPO}} = 0$ (■), 0.1 (●), 0.3 (▼), 0.5 (◄), 0.7 (►). [Surf.]T = 0.05 M.